Int. J. Heat Mass Transfer. Vol. 15, pp. 599–617. Pergamon Press 1972. Printed in Great Britain

A THEORETICAL INVESTIGATION OF THE EFFECT OF MASS TRANSFER ON HEAT TRANSFER TO AN EVAPORATING DROPLET

T. W. HOFFMAN and L. L. ROSS†
McMaster University. Hamilton. Ontario. Canada

(*Received* 17 *December* 1970 *and in revised form* 16 *June* 1971)

Abstract—A theoretical investigation was carried out on the interaction of the radial flow arising from mass transfer and the forced-convection flow field around an evaporating droplet in order to elucidate the effect of mass transfer on heat transfer.

The theoretical model was based on:

(i) uniform mass efflux around the droplet
(ii) error-distribution solution of the momentum equation
(iii) integral boundary-layer formulation of the energy equation.

The solutions for the case of zero mass efflux gave good agreement with previously reported correlations for $0 \leqslant Re \leqslant 1000$. Excellent agreement was found between the model and the available experimental data covering relatively high mass-transfer rates.

NOMENCLATURE

A_{mn}, constants in trial streamline function;
ANG, angular conduction terms in energy equation;
B', non-dimensional Spalding transport number, equation (5);
C_p, specific heat at constant pressure;
D, droplet diameter;
$\mathscr{D}^2$, mathematical operator, equation (1);
F_1, F_2, general functional relationships;
h, heat-transfer coefficient;
k, thermal conductivity;
m, exponent on Prandtl number in correlating equation (22) also subscript and integer exponent in trial streamline function;
$\dot{m}$, rate of evaporation of droplet;
Nu, non-dimensional Nusselt number, hD/k;
Nu_0, Nusselt number in absence of evaporation;
Nu_θ, Nusselt number corresponding to total transfer from $\theta = 0$ to $\theta = 0$;
$Nu(\theta)$, Nusselt number, point value at angular position θ;
n, exponent on Reynolds number in correlating equation (22) also subscript and integer exponent in trial streamline function;
Pe, non-dimensional Péclét number $DU_\infty \rho C_p/k$;
Pr, non-dimensional Prandtl number, $C_p\mu/k$;
$Pn(\cos\theta)$, nth order Legendre polynomial;
$Pn'(\cos\theta)$, first derivative of the nth order Legendre polynomial with respect to $\cos\theta$;
$q_2, q_3, \ldots, q_9$, functions pertaining to energy equation (derivation and listing available in Appendix C in [27]);

† Present address: C. F. Braun and Co., California. U.S.A.

Re, non-dimensional Reynolds number, $D U_\infty \rho/\mu$;
Re_I, Reynolds number based on injection velocity;
r, non-dimensional radial distance;
T, dimensionless temperature;
t, temperature;
U, fluid velocity;
V_s, interfacial radial velocity;
V_θ, angular velocity component;
V_r, radial velocity component;
x, $(1 - \cos\theta)$;
y, non-dimensional thermal boundary-layer thickness;
y^*, non-dimensional thickness at frontal stagnation point.

Greek letters

$\gamma(B')$, mass transfer shielding function;
θ, angular spherical coordinate;
λ, latent heat of vaporization;
μ, viscosity of flowing fluid;
ρ, density of flowing fluid;
$\phi(\theta)$, non-dimensional surface efflux parameter V_s/U_∞ at any angle θ;
ϕ_A, non-dimensional surface efflux parameter, independent of position;
ψ, non-dimensional streamline function.

Subscripts

∞, free stream values;
S, pertaining to surface;
θ, r, pertaining to any coordinate θ, r respectively.

THE WORK described in this paper is part of a study directed toward obtaining a quantitative understanding of the effect of vapour efflux on the heat transfer to an evaporating droplet. In particular the specific problem of interest is the interaction of the mass efflux with the forced-convection flow field around a droplet.

This phenomena is important in many spray processes such as spray drying, liquid fuel combustion, cyclone evaporation and the Atomized Suspension Technique [1] where the carrier gas and/or surrounding enclosure are maintained at high temperatures. Under these conditions the droplets are subjected to intense heat loads through conduction/convection and radiation from the surrounding gases and the enclosure surfaces. This results in relatively large rates of evaporation and hence a relatively large radial interfacial velocity. A theoretical investigation of the interacting flow fields and the heat transfer process coupled with experimental verification should provide a sound basis for extrapolating heat-transfer correlations to conditions well outside the limits which were used in formulating them.

INTRODUCTION

A critical review of previous investigations provided a basis for suitable simplifying assumptions thus reducing the complexity of the the problem, viz:

(i) The effects of natural convection are negligible compared to those of forced convection [2–5]
(ii) fluid properties may be considered uniform and evaluated at some pertinent reference temperature [6, 7]
(iii) shear-induced droplet circulation is negligible [8–10]
(iv) droplet evaporation may be considered a quasi steady-state process, i.e. the velocity and temperature fields are insignificantly different from those which exist if the droplet were not changing size [11, 12]
(v) the controlling resistance to transfer is in the external fluid phase [12, 13]
(vi) viscous dissipation, turbulence, compressibility and rarefaction effects are negligible [14].

Application of these assumptions to the general conservation of momentum and energy equations allows the phenomena of convective heat and mass transfer from a droplet to be expressed as [15]:

The momentum equation:

$$\frac{Re}{2}\left\{\frac{\partial\psi}{\partial r}\cdot\frac{\partial}{\partial\theta}\left(\frac{\mathscr{D}^2\psi}{r^2\sin\theta}\right)-\frac{\partial\psi}{\partial\theta}\cdot\frac{\partial}{\partial r}\times\left(\frac{\mathscr{D}^2\psi}{r^2\sin^2\theta}\right)\right\}\sin\theta-\mathscr{D}^4\psi=0 \quad (1)$$

where $\mathscr{D}^2=\frac{\partial^2}{\partial r^2}+\frac{\sin\theta}{r^2}\frac{\partial}{\partial\theta}\left(\frac{1}{\sin\theta}\frac{\partial}{\partial\theta}\right)$

$$V_\theta=+\frac{1}{r\sin\theta}\frac{\partial\psi}{\partial r};\qquad V_r=-\frac{1}{r^2\sin\theta}\frac{\partial\psi}{\partial\theta}$$

$$r=\frac{2r'}{D};\qquad \psi=\frac{4\psi'}{U_\infty D^2}.$$

The energy equation:

$$V_r\frac{\partial T}{\partial r}+\frac{V_\theta}{r}\frac{\partial T}{\partial\theta}=\frac{2}{Re\,Pr}\left\{\frac{1}{r^2}\frac{\partial}{\partial r}\left[r^2\frac{\partial T}{\partial r}\right]+\frac{1}{r^2\sin\theta}\frac{\partial}{\partial\theta}\left[\sin\theta\frac{\partial T}{\partial\theta}\right]\right\} \quad (2)$$

where

$$T=\frac{t-t_\infty}{t_s-t_\infty}$$

boundary conditions:

$$\text{at } r=1,\ V_\theta=0,\ V_r=\phi(\theta),\ T=1 \quad (3)$$
$$\text{at } r=\infty,\ V_\theta=\sin\theta,\ V_r=-\cos\theta,\ T=0$$

and $\phi(\theta)=\left(\frac{V_s}{U_\infty}\right)_{(\theta)}$.

In two component systems the conservation equations for the diffusing components should be considered as well to determine the droplet temperature. On the other hand, at the relatively high temperature differences where this analysis is important, the droplet does not vary appreciably with the temperature of the surroundings [16, 17]; moreover, the percentage error in the temperature driving force is expected to be very small. Therefore we will assume that the droplet temperature is known *a priori*.

The prediction of the overall heat-transfer rate through the dimensionless Nusselt number, is given by

$$Nu=-\int_0^\pi(\partial T/\partial r)_{r=1}\sin\theta\,d\theta=F_1[Re, Pr, \phi(\theta)] \quad (4)$$

requires the simultaneous solution of equations (1) and (2) with the boundary conditions (3). The equations are coupled through the interfacial velocity term $\phi(\theta)$.

Attempts to find a functional relationship F_1 using various simplified models and empirical data have appeared in the literature over the past two decades and have been discussed in [18].

It would appear that the theoretical approach for elucidating the form of F_1 exactly by simultaneously solving equations (1) and (2) would require extensive computational facilities and excessive computer time. Moreover, severe difficulties have been experienced in attempts to simultaneously solve the momentum and energy equations by finite-difference techniques [19]. Therefore a suitable approximation is clearly indicated.

The analysis of previous work has suggested an additional assumption which may be suitable in most cases of practical interest; certainly it permits a significant simplification of the problem. This assumption may be stated as follows: The surface flux interaction of the momentum and heat transfer processes is characterized primarily by the level of mass transfer rather than its angular distribution; the effect of angular distribution is considered second-order and therefore neglected. Thus it is permissible to select a uniform surface-flux distribution for purposes of analysis (i.e. $\phi(\theta)=\phi_A=$ constant.

A uniform dimensionless surface flux, ϕ_A, may be expressed in terms of more easily measured parameters. For example, use of an energy balance over the surface of the drop yields:

$$\phi_A=\frac{1}{2}\int_0^\pi\phi(\theta)\sin\theta\,d\theta=\frac{Nu\,B'}{RePr} \quad (5)$$

where

$$B'=\frac{C_p(t_\infty-t_s)}{\lambda-\frac{q_R}{\dot m}},$$

is the dimensionless Spalding transport number representing the ratio of the sensible heat requirements to the convective heat load. With this assumption of uniform surface flux

$$Nu = F_2(Re, Pr, B'). \tag{6}$$

The functional form of F_2 may be established by simply solving the momentum equation for various values of Reynolds number and surface flux and substituting the appropriate velocity and Prandtl number in the energy equation.

FORMULATION OF MODEL

Since the system of equations is not amenable to an exact solution, approximate methods must be employed. The same approach need not necessarily apply to both equations.

In choosing an approximate method of solution, the following criteria were established:

(i) maximum accuracy in the Reynolds number range from about 20 to 500. This is the region where experimental verification of the method is easily achieved.

(ii) maximum accuracy of the hydrodynamics and temperature gradient near the surface of the sphere.

(iii) description of the whole velocity field including the wake region.

(iv) amenable to a boundary condition involving a finite interfacial velocity.

(v) correct convergence of the solution to the asymptotic values

$$\lim Nu = 2 \quad Re \to 0 \quad \phi_A \to 0 \tag{7}$$

and

$$\lim Nu = 0 \quad Re \to 0 \quad \phi_A \to \infty \tag{8}$$

(vi) relatively straight forward solution technique which does not require excessive computer time and facilities.

(vii) analytical representation of the velocity profile is necessary since the energy requires velocity components at every point in its solution.

TREATMENT OF THE MOMENTUM EQUATION

The available treatments for the hydrodynamics solution may be classified as: Stokes, potential flow, boundary-layer and the Galerkin error-distribution method.

Stokes solution satisfies all the conditions but is only applicable at very low Reynolds number: potential flow solutions [21] are not accurate near the surface; boundary-layer solutions especially that employed by Frössling [11] are not readily amenable to a finite interfacial-velocity boundary condition; Spalding's approximate boundary-layer methods [22] are well-suited to this condition but these solutions apply only up to point of separation and their applicability to low Reynolds numbers especially under conditions of surface flux is questionable.

Kawaguti's use [23] of Galerkin's error distribution method [24] yields the most satisfactory results in the Reynolds number range of interest. Its application to the case under consideration here has already been reported [18]. Basically it consists of choosing trial streamlines of the form,

$$\psi = \frac{1}{2} r^2 \sin^2\theta + \sum_{n=1}^{\infty}\sum_{n=1}^{\infty}\left\{\frac{A_{mn}}{r^m}\sin^2\theta\, P_n'(\cos\theta)\right\} + \phi_A(\cos\theta - 1) \tag{9}$$

and then evaluating the constants so as to satisfy the boundary conditions and minimize the error over the remaining flow field. Once the constants of the stream function are evaluated the velocity components at every point are known and these values can be used in the solution of the energy equation.

In the present study, the series for the trial streamline function was truncated at $m = 4$ and $n = 2$; the details are presented in [18].

TREATMENT OF THE ENERGY EQUATION

As in the case of the momentum equation, no exact solution is available for the complete

energy equation in spherical coordinates. A review of the literature indicates that aside from Yuges treatment [25] and finite difference methods [19], virtually all solutions have been obtained using boundary-layer formulations. Yuge's method may be excluded from consideration, not only because it is tedious and prone to truncation errors but also because it has not been proven to be convergent in the general case.

Boundary-layer formulations suffer from their inapplicability at lower Péclét numbers and beyond the separation point and their incorrect asymptotic Nusselt number for zero flow.

An integral boundary-layer approach has been suggested by Friedlander [26] in which the energy equation is expressed in integral form. The application of this integral method to the specific problem at hand is described below.

Consider a sphere located in a uniform forced-convection flow field of velocity, U_∞, in the negative x-direction. For the case of a uniform property fluid, no viscous dissipation, and axial symmetry, the complete energy equation may be expressed in integral form as [27].

$$\frac{\mathrm{d}}{\mathrm{d}\theta}\left\{\int_1^y T V_\theta r \sin\theta \,\mathrm{d}r - \frac{2}{Pe}\int_1^y \frac{\partial T}{\partial \theta}\cdot \sin\theta \cdot \mathrm{d}n\right\} = \frac{2}{Pe}\left\{-\frac{\partial T}{\partial r} + \frac{Pe\theta_A}{2}\right\}_{r=1} \sin\theta. \quad (10)$$

If angular conduction is negligible compared to angular convection, the second term on the left-hand side of equation (10) may be removed.

In this section solutions are obtained for equation (10) and the simplified one considering negligible angular convection. The hydrodynamic models discussed previously may be used to provide an analytic expression for the angular velocity term, V_θ. The pertinent boundary conditions are given as:

$$\text{at} \quad r = 1, {}^{(1)}\, T = 1, {}^{(3)}\, \frac{\partial^2 T}{\partial r^2} - \left(\frac{Pe\phi_A}{2} - 2\right)\frac{\partial T}{\partial n} = 0 \quad (11)$$

$$\text{at} \quad r = y, {}^{(2)}\, T = 0, {}^{(4)}\, \frac{\partial T}{\partial r} = 0$$

where y is the dimensionless thermal boundary-layer thickness which is a function of θ.

SOLUTION OF MODEL

A general solution of equation (10) in terms of the dimensionless temperature distribution, $T(r, \theta)$, is intractable at the present time. Here a suitable polynomial representation of temperature distribution is chosen†, the constants associated with the polynomial are evaluated by applying the pertinent boundary conditions, equation (11). The suitability of the polynomial form is dictated by its conformity with the following requirements:

(i) boundary conditions must be independently satisfied.
(ii) no discontinuities can occur within the boundary layer.
(iii) The local Nusselt number asymptotically must approach that for pure radial conduction with increasing boundary-layer thickness

$$\text{i.e.} \left(\frac{\partial T}{\partial r}\right)_{r=1} \to -1 \text{ as } y \to \infty.$$

Two temperature polynomial forms were found to satisfy requirements (i), (ii) and (iii), namely,

$$T = a + \frac{b}{r} + cr \qquad \text{Profile 1} \quad (12)$$

$$T = a + \frac{b}{r} + cr + dr^2 \qquad \text{Profile 2} \quad (13)$$

Profile 1 was made to satisfy only boundary

† The choice of other terms in the profile have a profound influence on the solution to extrapolate to the correct asymptotic values.

conditions (1), (2) and (3), equation (11), while the more rigorous Profile 2 satisfied all four conditions.† Substituting equation (13) into the boundary conditions (11) yields the constants a, b, c and d as functions of y, Pe and ϕ_A. Therefore it can be seen that if the boundary-layer thickness, y, is known as a function of the angle then the temperature field is defined at all points. This functional relationship is determined by substituting the temperature profile and velocity field into equation (10) and carrying out the indicated integrations and differentiations, viz:

$$(q_5 + q_6 \cos\theta)\sin\theta\frac{dy}{d\theta} = \frac{2}{Pe}(1 + F_3) - \{2q_2\cos\theta + (3\cos^2\theta - 1)q_3\} + \frac{2}{Pe}\left[q_7\frac{\cos\theta\, dy}{\sin\theta\, d\theta} + q_9\left(\frac{dy}{d\theta}\right)^2 + q_7\frac{d^2y}{d\theta^2}\right] \quad (14)$$

where‡ q_2, q_3, q_4, q_5, q_6, q_7, q_9 and F_3 are functions of y. The boundary conditions associated with equation (14) are:

$$\frac{dy}{d\theta} = 0 \qquad \text{at} \quad \theta = 0° \text{ and } 180°. \quad (15)$$

Equations (14) may be solved by numerical methods. Moreover, since it is a boundary value problem, recourse to an interative procedure is necessary.

If the angular conduction is small with respect to the angular convection, the angular conduction can be neglected and the problem reduces to an initial value problem which may be solved without iteration using the symmetry boundary condition at $\theta = 0$.

This solution, $y(\theta)$, may be used to generate an approximation of the neglected angular conduction terms. If this approximation is substituted into the complete energy equation (14) a second solution may be obtained. This solution may then be used to generate a better approximation for the angular conduction terms, thereby generating a third solution. This iteration scheme is illustrated mathematically by rewriting equation (14) as:

$$(q_5 + q_6\cos\theta)\sin\theta\frac{dy}{d\theta} - \frac{2}{Pe}(1 + F_3) + \{2q_2\cos\theta + (3\cos^2\theta - 1)q_3\} = \frac{2}{Pe}(ANG)_p \quad (16)$$

where the subscript p denotes the function evaluated from the previous iteration, and

$$ANG = q_7\frac{\cos\theta\, dy}{\sin\theta\, d\theta} + q_9\left(\frac{dy}{d\theta}\right)^2 + q_7\frac{d^2y}{d\theta^2}. \quad (17)$$

This iteration scheme is continued until the desired degree of convergence is obtained. This method has the advantage that the initial solution corresponds to the solution of the energy equation for the case of negligible angular conduction; successive iterations allow an evaluation of the importance of the angular conduction terms.

DETAILS OF SOLUTION

Consider the initial conditions associated with equation (16). The initial condition specifies that $dy/d\theta = 0$ at $\theta = 0$. It may be readily seen from equation (16), that for the solution sought,

$$\frac{2}{Pe}(1 + F_3) - 2(q_2 + q_3) + \frac{2}{Pe}(ANG)_p = 0 \text{ at } \theta = 0. \quad (18)$$

Therefore, solution of the algebraic equation (18) yields the starting value of y, namely, y^*.

The form of the energy equation is not satisfactory for numerical integration procedures because $dy/d\theta \simeq 0$ near the starting point, $\theta = 0$. This difficulty may be resolved by use of the co-ordinate transformation, $\cos\theta = 1 - x$.

† Further discussion is restricted to Profile 2; the interested reader is referred to [27] for solutions employing Profile 1.

‡ The interested reader is referred to Appendix C of [27] for a detailed derivation and listing of all the functions.

Equation (16) thus takes the form

$$\frac{dy}{dx} = \frac{[(2/Pe)(1 + F_3) - 2(q_2 + q_3)]/x + 2q_2 + 3(2 - x)q_3 + (2/Pe)(ANG)_p}{(2 - x)\{q_5 + (1 - x)q_6\}} \quad (19)$$

$$\text{where } ANG = \frac{2(1 - x)}{x} q_7 \frac{dy}{dx} + (2 - x) q_9 \left(\frac{dy}{dx}\right)^2 + (2 - x)q_7 \frac{d^2y}{dx^2}. \quad (20)$$

Boundary condition (18) may be expressed as

$$\frac{2}{Pe}(1 + F_3) - 2(q_2 + q_3) + \frac{2}{Pe}\left(q_7 \frac{dy}{dx}\right)_p = 0 \text{ at } x = 0. \quad (21)$$

Application of L'Hôpital's rule to the indeterminancy in equation (19) at $x = 0$ yields a starting value of dy/dx.

Expressions for the local and overall Nusselt number in terms of the pertinent parameters are derived in Appendix A.

The energy equation (10) or its alternatives, equations (19) and (21) were numerically integrated using a fourth-order Runge–Kutta process (28). The initial value of bounday-layer thickness, y^*, was accurately determined to six figures using a Bolzano iterative solution (27) of the equation (21).

DISCUSSION OF THE THEORETICAL MODEL

From the frontal stagnation up to the flow separation point all the flow lamina are moving in the direction of increasing angle (measured from the frontal stagnation point). Thus, if the angular conduction-transfer component is neglected, the convection heat-transfer rate at a particular point on the sphere in this unseparated flow region does not depend on conditions downstream from that point. Furthermore, in this region the assumption of "similar" temperature-profiles should be satisfactory, as the flow field is quite similar to boundary-layer flow. It is not expected, however, that the polynomial temperature profiles would give a precise representation over the whole fluid region; accurate results would be expected only close to the sphere surface because the two boundary conditions are satisfied there. It should be noted that, at the flow separation point, the zero-surface-vorticity condition forces the local Nusselt number to a value close to 2·0 which would be expected on physical grounds.

Extension of the "marching" solution past the flow separation point presents problems, both in the validity and the physical interpretation of the integration procedure. At present, no solutions are available for the temperature distribution in the wake region. Since this region consists, in part, of a region of reverse flow (i.e. flow from the rear stagnation point toward the flow separation point), the assumption that the transfer at a particular point is independent of downstream conditions is no longer valid. The "similar"-temperature profile assumption is questionable in this region as well. Nevertheless, the marching solution was extended forward through the vortex region to the rear stagnation point. Hamielec [30] suggested that there should be an inward flow of fresh fluid at the rear stagnation point; no account of this was made here. With these assumptions it was found that the Nusselt number asymptotically approached a value of 2·0. Under these conditions, the contribution of the wake region to the overall process is only about 10 per cent; thus, an approximate determination should not significantly affect the value of the overall Nusselt number.

ASYMPTOTIC SOLUTIONS OF THE ENERGY EQUATION

Two asymptotic energy transfer regimes permit a number of simplifying assumptions to be made which result in analytic expressions for the overall Nusselt numbers. The regimes are those of high energy transfer (thin boundary

layer) and low energy transfer (thick boundary layer). These two cases are solved in Appendix B.

RESULTS

(a) *Importance of the angular conduction term*

In order to estimate the importance of the angular conduction term, the complete energy equation (10) was solved over a range of Reynolds numbers for the case of $\phi_A = 0$, $Pr = 1{\cdot}0$, using the iteration-solution scheme outlined previously. The local Nusselt number was not found to change significantly (< 5 per cent) with successive iterations even at low Reynolds numbers.

Unfortunately, at very low Reynolds numbers ($Re \simeq 0$), this iterative scheme not only required a large number of iterations but was also unstable.

(b) *Solutions at low Péclét numbers*

The complete energy equation becomes more and more elliptic in nature with decreasing Péclét number. In the low Péclét number region the angular conduction transfer is no longer negligible with respect to the angular convection transfer. Therefore, ignoring it should result in inaccurate solutions.

Consider the case of a Prandtl number of unity and a Reynolds number regime of less than unity. As the Stokes hydrodynamic model [20] should be applicable, the various "exact" solutions employing this model [31–33] may be compared to the present solutions (single iteration). This comparison is shown in Table 1.

Table 1. Predicted Nusselt numbers using various models

N_{Pe}	[32]	[31]	[33]	[26]	[37]	This model†
0·1	2·055	2·053	2·044	2·043	2·049	2·0533
0·2	—	—	—	—	—	2·1013
0·5	2·284	2·326	2·209	2·163	2·182	—
1·0	2·467	2·803	2·534	—	—	2·3850
2·0	—	—	—	2·438	2·477	—

† $Pr = 1$.

The satisfactory agreement of the present solution with the various exact solutions seems at first glance fortuitous, as the angular conduction mechanism is significant in this region. However, examination of the present theoretical treatment reveals that the satisfactory results obtained in this low Péclét number region may be attributed almost wholly to the judicious choice of temperature profile. In particular, the additional requirement, that local value of radial temperature derivative at the sphere surface approach the exact solution as the thermal boundary layer becomes infinitely thick, forces the "no-angular conduction" solution to approach the exact solution as the Péclét number is decreased to zero. In other words, as the Péclét number approaches zero, the present "no-angular conduction" solution deviates from the correct no angular conduction solution in such a manner as to asymptotically approach the correct solution of the complete energy equation.

(c) *Theoretical solutions (zero mass efflux, $\phi_A = 0$)*

Figure 1 shows the results obtained for the case of $\phi_A = 0$. Also shown is the thick boundary-layer solution.

As the Reynolds number is decreased, the model, as expected, merges smoothly with its asymptotic analytic solution. It is seen that, even at a Péclét number of unity, the thick boundary-layer solution has diverged considerably.

The solutions at different Prandtl numbers yield a family of curves having almost parallel slopes on the log–log plot of Fig. 1. These solutions may be used to investigate the Prandtl number dependence of the results. As the regime of primary interest in the present study pertains to that of a gaseous medium, only the range of Prandtl number from 0·7 to 10·0 has been considered in the following analysis.† The results indicate that over a sufficiently narrow Prandtl and Reynolds number range, the form

† A number of high Prandtl number solutions were obtained (i.e. $Pr = 1000$) over the Reynolds number regime $1 < Re < 500$. These were found to be in excellent agreement with various boundary-layer solutions.

of the energy transfer relationship may be given as,

$$Nu = 2 + ARe^n Pr^m. \quad (22)$$

The results were applied to equation (22) to produce values of the exponent m as a function of Prandtl number and Reynolds number.

For a given Prandtl number the exponent, m decreased with increasing Reynolds number. The exponent was also seen to decrease slightly with increasing Prandtl number. (This latter behaviour is less pronounced at higher Reynolds numbers.) The "thick" boundary-layer analytic solution predicts a Prandtl number exponent of unity in the low Péclét number regime. On the other hand, the "thin" boundary-layer solution predicts as exponent of one-third for high Péclét numbers.† Therefore, one should expect a decreasing value of Prandtl number exponent with increasing Péclét number, its value approaching one-third in the region of bounday-layer transfer. This is exactly the trend shown by the results.

† This is in agreement with boundary-layer results for high Reynolds numbers [11].

If it is assumed that over the Prandtl number range of interest that the exponent m is only a function of the Reynolds number, the following correlation of the data results:

$$m = \tfrac{1}{3} + \tfrac{2}{3}\exp(-0{\cdot}85\, Re^{0{\cdot}24}). \quad (23)$$

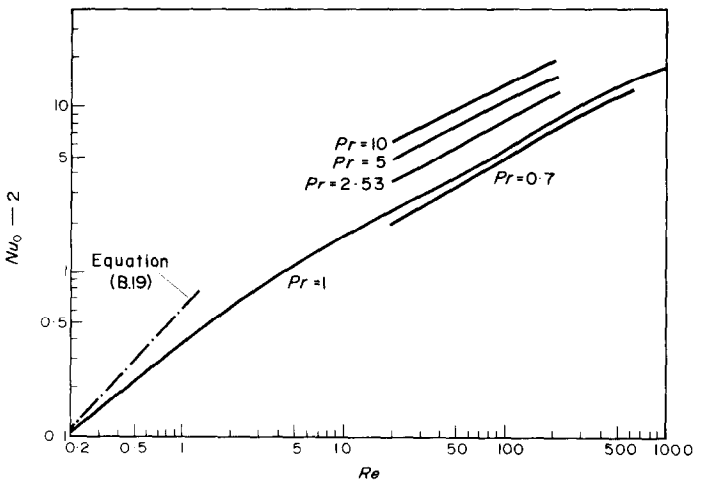

FIG. 1. Nusselt number as a function of Reynolds number for heat transfer only: mass transfer is negligibly small. Prandtl number is the parameter on each curve.

The form of equation (23) has been chosen to yield the proper asymptotic values of m, namely, 1 and $\frac{1}{3}$. The approximate dependence of the Reynolds number exponent, n, on the Reynolds number may be evaluated from the present results using equation (22). This dependence is shown graphically in Fig. 2. As the Reynolds number is decreased below 20, the exponent increases, while above a Reynolds number of about 200 the exponent decreases continuously to the asymptotic value of $\frac{1}{3}$ predicted by the present "thin" boundary-layer solution. The trend at low Reynolds numbers may be easily explained, in that, as the Reynolds number is decreased, the exponent must increase and approach the value of unity predicted by the thick boundary-layer asymptote.

Figure 3, which shows the angular distribution of heat transfer, allows a detailed examination of the heat-transfer phenomena. Also

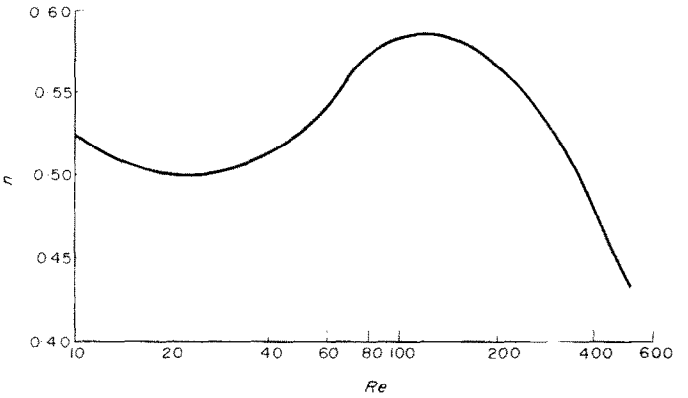

FIG. 2. The variation of the Reynolds number exponent in equation (22) with Reynolds number.

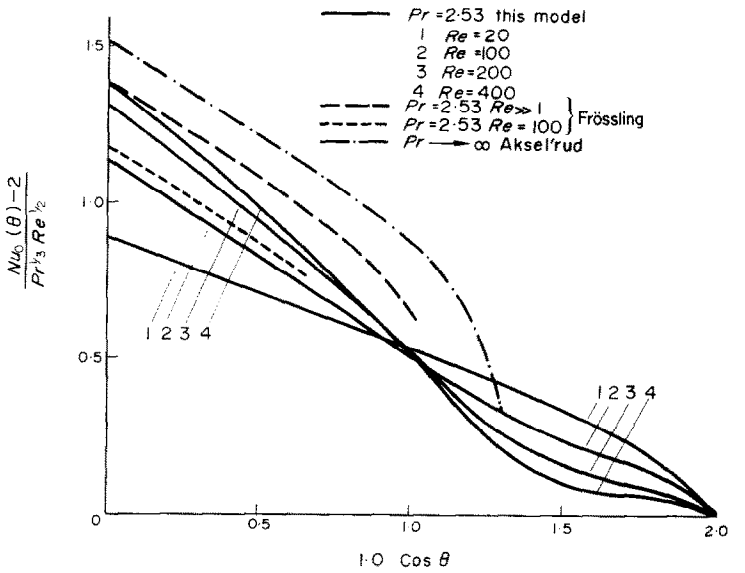

FIG. 3. Predicted angular distribution of heat transfer. Comparison of predictions of this model with those of boundary layer solutions of Frössling [11] and Aksel'rud [35].

shown, is the boundary-layer solution of Frössling [11] for the case of $Pr = 2{\cdot}53$. For purposes of comparison with this solution, the present model has also been evaluated at the same Prandtl number.

As the value of the Prandtl number exponent, m, equation (23), was found to be about one third, the normalized heat-transfer parameter which was used for the ordinate of Fig. 3 tends to bring all Prandtl number solutions together.†

The abscissa in Fig. 3, $(1 - \cos\theta)$ has been

† For the case of Frössling's and Aksel'sud's solutions, the Nusselts number approached zero asymptotically as the Reynolds number was decreased. Therefore for their solutions $Nu(\theta)$ rather than $Nu(\theta) - 2$ has been used in the ordinate of Fig. 3.

chosen so that the area under the curve from 0 to $(1 - \cos\theta)$ is proportional to the transfer rate over the surface of the sphere from $\theta = 0$ up to $\theta = \theta$. Thus, the various solutions can be used directly to compare relative rates of transfer over the surface of the sphere.

The solutions show a consistent trend, with the relative heat transfer contributions increasing over the frontal and decreasing over the rear portions of the sphere surface as the Reynolds number is increased. It has been shown previously [29] that both the frontal-region dimensionless surface vorticity and the size of vortex ring increase with increasing Reynolds number. The former phenomena accounts for the increase in frontal-region heat transfer rate.

The results shown in Fig. 3 indicate that the overall heat transfer process is controlled by the frontal transfer contribution. In the separated flow regime, the contribution of the wake transfer to the overall transfer process is about 12 per cent.

On the whole, the present solutions seem to be in satisfactory agreement with Frössling's boundary-layer solution. This solution is only strictly valid for rather high Reynolds numbers (for the case of a gaseous fluid). Therefore, as expected, the present theoretical results approach Frössling's solution as the Reynolds number is increased.

The theoretical analysis of the heat-transfer process is amenable to various simplifications at the frontal stagnation point: this has resulted in a number of reliable boundary-layer treatments. These are compared with the present results in Fig. 4. The solution at $Re = 200$ is in excellent agreement with the solutions of Frössling [11], Sibulkin [34] and Aksel'rud [35].

The regime of validity of the present model may be determined by comparison with various available experimental and theoretical studies. Aside from the Stokes flow regime, which has been already discussed, most theoretical treatments have employed the boundary-layer assumptions which are not strictly valid in the Reynolds number regime of present interest, namely, $Re < 500$. These boundary-layer solutions may, however, be used to predict the upper Reynolds number limit of applicability of the present theory.

Because of this lack of pertinent theoretical solutions, recourse has been made to a number of experimental studies. Critical evaluation of these studies [18, 27] has enabled what is felt to be the most reliable correlations to be selected [2, 11, 12, 35]. These results, along with the present solution, are shown in Fig. 5.

The present theory is seen to be in good agreement with the various correlations over entire Reynolds number range.

Consider the lower Reynolds number range, that is, $Re < 500$. The correlation of Ranz [12] lies about 10 per cent above the Yuge [2] and Frössling [11] line† which in turn predicts

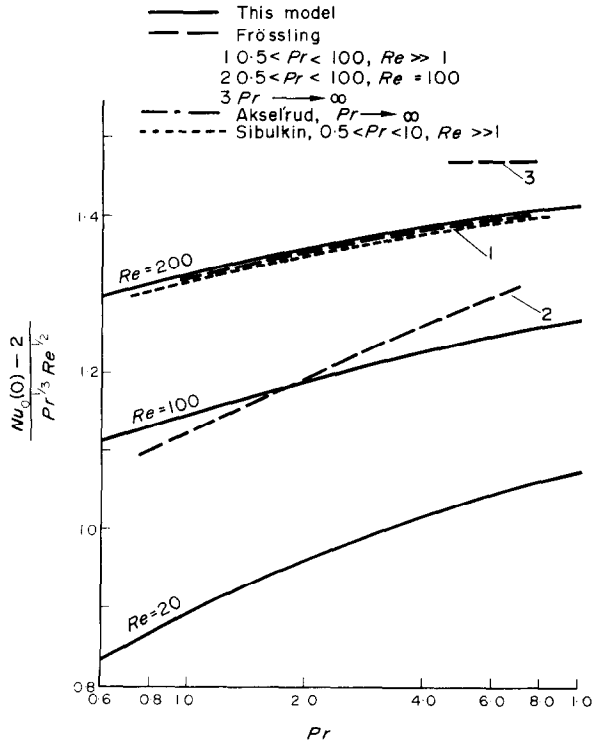

FIG. 4. Comparison of predicted results for heat transfer at the frontal stagnation point (negligible mass transfer).

† Yuge's and Frössling's correlations are virtually the same and so have been represented as a single line on Fig. 5.

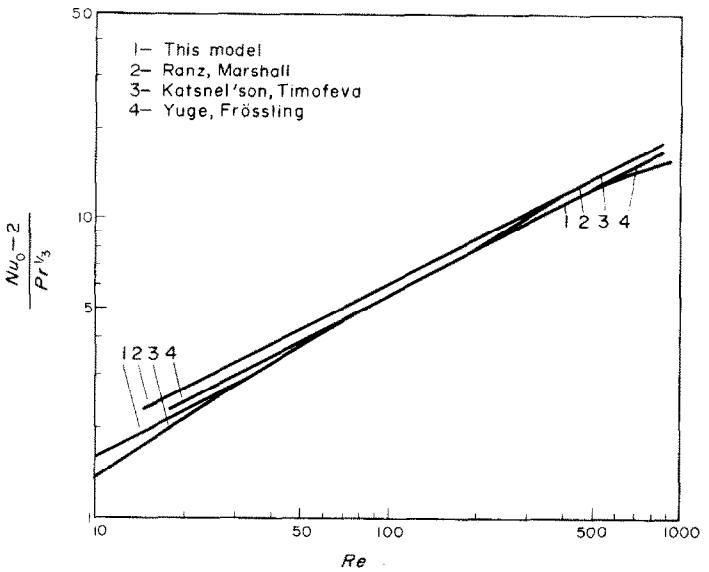

FIG. 5. Comparison of various correlating equations with the calculated results over Reynolds number range of interest.

slightly higher Nusselt numbers than the present theory for Reynolds numbers below 100.

Except for the correlation of Katsnel'son [36] which is in excellent agreement with the present results, the correlations have been obtained using a Reynolds number exponent of 0·5. As shown on Fig. 2, the present model exhibits a rather sharp increase in exponent above the value of 0·5 around a Reynolds number of 100.

It has been shown [19] that the present hydrodynamic model was unsatisfactory above Reynolds numbers of about 500. This, in turn, causes the angular heat transfer distribution to diverge from the expected asymptote, namely, Frössling's boundary-layer solution. This behaviour is reflected in the overall transfer results plotted in Fig. 5; however, the deviation is small even at Reynolds number above 500.

(d) *Effect of mass transfer on heat transfer*

One of the primary aims of the theoretical program was to investigate the effect of surface flux (i.e. mass transfer) on the heat-transfer process. This interaction phenomenon is characterized by the modified Spalding transport number, B'.

The present results are shown on Fig. 6. The $B' = 0$ solution is, of course, the zero-mass efflux solution discussed in the previous section. The effect of increasing the sensible heat shielding around the sphere, that is, increasing the B' parameter, is to displace the heat transfer curve; its shape remains essentially the same. Figure 7 shows the effect of the mass efflux on the local heat-transfer process for the case of $Re = 100$ and $Pr = 1{\cdot}0$.

It is of interest at this point to determine an analytic expression that will satisfactorily represent the effect of mass efflux on the heat process. Figures 6 and 7 indicate that the effect of the Spalding number on the heat transfer vs. Reynolds number or angle relationship is to shift the zero-mass efflux curve rather than radically change its shape. In other words, the effect of the Spalding number on the transfer rate is virtually independent of the Reynolds number. In [19] it is shown that the streamlines around the droplet are not affected appreciably by a varying mass efflux but depend strongly

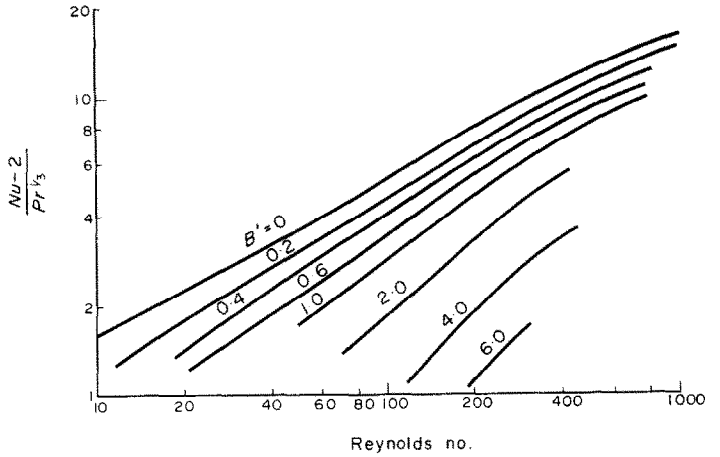

FIG. 6. The effect of mass transfer on Nusselt number vs. Reynolds number relationship.

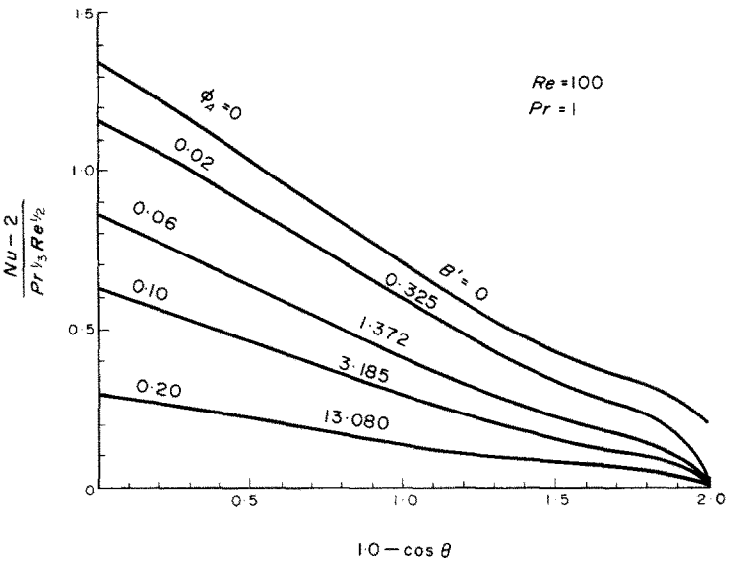

FIG. 7. The effect of mass transfer on the angular distribution of heat transfer (Reynolds number = 100; Prandtl number = 1).

upon the magnitude of the flux. This indirectly suggests that the effects noted above are not a result of the assumption of constant mass efflux over the surface. This, in turn, suggests that the convective heat-transfer parameter, i.e. the Nusselt number, may be expressed in the forms,

$$Nu = Nu_0^* \, Pr^m \, \gamma(B') \tag{24}$$

where Nu_0^* is the Nusselt number when the Prandtl number is unity and the driving force

B' vanishes. The expression, $\gamma(B)$, which is commonly referred to as the mass-transfer shielding, is only a function of the Spalding number. For the case of a known Prandtl number dependence, equation (24) may be rewritten as,

$$\frac{Nu}{Nu_0} = \gamma(B').$$

Equation (25) suggests that, if the theoretical results are plotted as indicated, the grouping, Nu/Nu_0, should only be a function of the Spalding number. Figure 8 shows a plot for the overall efflux in heat transfer over the flow regime of present interest was carried out [18]. The data were subjected to a rigorous regression analysis and the resulting correlation was virtually identical with the results of the present theoretical model over the range $20 < Re < 200$. The excellent agreement confirms the validity of the assumptions made in the formulation of the theoretical model.

CONCLUSION

Solutions of the present model for the case of negligible angular conduction term† are in

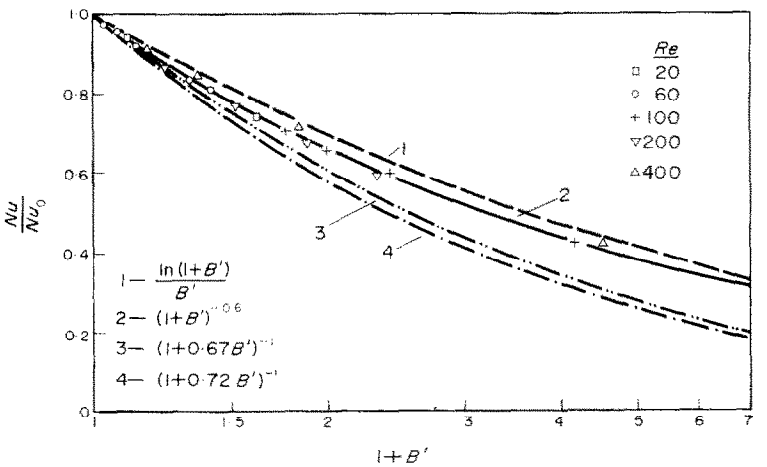

FIG. 8. Effect of mass efflux on heat transfer—comparison of the various analytical mass transfer shielding expressions with results calculated from this model. (Note: calculated results from this model at various Reynolds numbers appear at points, +, ○, □, ▽, △, at Re = 20, 60, 100, 200, 400 respectively.)

transfer rates. Also plotted are shielding functions that have been used in previous studies. The results tend to confirm the validity of equation (25). The satisfactory correlation is quite remarkable considering the range of Reynolds and Spalding numbers covered.

No satisfactory theoretical solutions are available for direct comparison with the present solutions, as most are based on boundary-layer which has been shown to be invalid in the regime of primary interest, namely, $0 < Re < 500$.

An experimental study on the effect of mass

excellent agreement with exact solutions of the complete energy equation in the low Péclét number regime. As the angular conduction transfer mechanism is obviously important in this regime, the satisfactory results must be attributed almost wholly to the judicious choice of temperature polynomial form (i.e. as the Péclét number is decreased to zero, the local heat-transfer rates reduct to the correct asymp-

† This corresponds to the first-iteration solution.

totic values predicted by a pure radial conduction transfer mechanism).

On the whole it may be concluded that the first-iteration solutions of the energy equation yields good results in the low Péclét number regime. Therefore higher-order iteration solutions are unnecessary.

The effect of both the Prandtl and Reynolds numbers on the Nusselt number was investigated. The present theory indicates that the Prandtl number exponent, m, is primarily a function of the Reynolds number; the results are satisfactorily correlated by equation (23).

The Reynolds number exponent, n, also depends on the Reynolds number. At low Reynolds numbers the exponent asymptotically approaches a value of unity. As the Reynolds number is increased, the exponent decreases; however, the limitations inherent in the hydrodynamic model at Reynolds numbers above 500 causes the exponent to diverge from the value of $\frac{1}{2}$ predicted by boundary-layer theory toward a value of $\frac{1}{3}$.

As the Reynolds number increases, the local heat-transfer rates as predicted by the present model approach the values obtained by the boundary-layer solutions of Frössling and Aksel'rud. The lower Reynolds number limit of applicability of the boundary-layer solutions is well above 200. Comparison of the frontal stagnation point transfer rates with other theoretical results offers additional confirmation of the validity of the present model.

The overall transfer rates predicted by the present model are in excellent agreement with reliable experimental correlations over the Reynolds number range, $20 < Re < 500$. The divergence of the higher Reynolds results caused by the breakdown of the hydrodynamic model is small. Furthermore, the differences between the experimental and predicted results in the low Reynolds number region (i.e. $Re < 20$) is insignificant in view of the uncertainty of the experiment data in this region. The present theory also results in satisfactory predictions of overall Nusselt numbers in the very low Reynolds number region (i.e. $Re < 1$). It may therefore be concluded that the present theoretical model yields a satisfactory representation of the overall heat transfer process over the Reynolds number regime $0 < Re < 500$.

Mass transfer causes a decrease in the convective heat-transfer rate, the relative decrease being virtually independent of the Reynolds number and being a function only of the Spalding number. The overall effect can be represented by a series of parallel curves of Nusselt number vs. Reynolds number with Spalding number as a parameter. This characteristic indicated that the present shielding results may be correlated as a function of only the Spalding number. This correlation was found to be in excellent agreement with a number of analytic shielding expressions obtained using highly idealized hydrodynamic fields and geometries.

The satisfactory agreement of the present results with experimental data seems to substantiate the assumption that the primary parameter characterizing the shielding phenomena is the level of the mass efflux rather than its angular distribution.

The present model may be used to provide a confident extrapolation of experimental data to other Reynolds number regimes and/or systems of interest.

ACKNOWLEDGEMENTS

Financial support for this project was supplied by the National Research Council of Canada and The Pulp and Paper Research Institute of Canada. One of us (L.L.R.) gratefully acknowledges N.R.C. and Shell Oil Scholarships which he received during this program.

Professor A. E. Hamielec provided many very useful suggestions during the course of this work.

REFERENCES

1. W. H. Gauvin and J. J. O. Gravel, Chemical reaction in solids–gas conveyed systems, Proc. Symposium on the Interaction between Fluids and Particles, pp. 250–259. Inst. Chem. Eng., London (1962).
2. T. Yuge, Experiments on the heat transfer from spheres including combined natural and forced convection. *J. Heat Transfer* **80C**, 214–220 (1960).
3. F. H. Garner and R. B. Keey, Mass transfer from single solid spheres. *Chem. Engng Sci.* **9**, 119–129 (1958).

4. L. I. KUDRYASHEV and L. YA. IPATENKO, Effect of free convection on the heat transfer coefficient for flow around a sphere at low Reynolds numbers, *Zh. Tekh. Fiz.* **29**, 309–312 (1959).
5. D. C. T. PEI, C. NARASIMHAN and W. H. GAUVIN, Evaporation from drop and particle in high temperature surroundings, Proceedings of the Symposium on the Interaction between Fluids and Particles, pp. 243–249, Inst. Chem. Eng. London (1962).
6. E. R. G. ECKERT, Engineering relations for heat transfer and friction in high velocity laminar and turbulent boundary layer flow over surfaces and constant pressure and temperature, *Trans. Am. Soc. Mech. Engrs* **78**, 1273–1283 (1956).
7. M. F. ROMIG, Stagnation point heat transfer for hypersonic flow, *Jet Propulsion* **26**, 1098–1101 (1956).
8. F. H. GARNER and D. HAMMERTON, Gas absorption from single bubbles *Trans. Inst. Chem. Engrs* **32**, S18–S24 (1954).
9. F. H. GARNER and A. H. P. SKELLAND, Some factors affecting droplet behaviour in liquid–liquid systems, *Chem. Engng Sci.* **4**, 149–158 (1955).
10. A. I. JOHNSON and L. BRAIDA, The velocity of fall of circulating and oscillating liquid drops through quiescent fluids *Can. J. Chem. Engng* **35**, 165–172 (1957).
11. N. FRÖSSLING, Evaporation, heat transfer and velocity distribution in two dimensional and rotationally symmetrical laminar boundary layer flow NACA TM 1432, Washington, D.C. (1958).
12. W. E. RANZ, Evaporation of drops, Ph.D. Thesis, Chem. Eng. Dept., University of Wisconsin (1950); see also, *Chem. Engng Prog.* **48**, 141, 173 (1952).
13. R. J. PRIEM, G. L. BORMAN, M. M. EL WAKIL, O. A. UYEHARA and P. S. MYERS, Experimental and calculated histories of vaporizing fuel droplets, NACA TN 3988 (August 1957).
14. H. SCHLICHTING, *Boundary Layer Theory*. McGraw-Hill, New York (1955).
15. R. B. BIRD, W. E. STEWART and W. LIGHTFOOT, *Transport Phenomena*, Chapter 4. John Wiley, New York (1962).
16. K. KOBAYASI, *Combustion of a fuel droplet, Fifth Symposium on Combustion*, pp. 141–148, Butterworth, London (1955).
17. T. W. HOFFMAN and W. H. GAUVIN, Evaporation of stationary droplets in a high temperature surroundings *Can. J. Chem. Engng* **38**, 129–137 (1960).
18. L. L. ROSS and T. W. HOFFMAN, Evaporation of droplets in a high temperature environment, Proceedings of Third International Heat Transfer Conference, V. 50–59 (1966).
19. A. E. HAMIELEC, T. W. HOFFMAN and L. L. ROSS, Numerical solution of the Navier Stokes equation for flow past spheres, *A.I.Ch.E. Jl* **13**, 212–219 (1967).
20. G. G. STOKES, *Mathematical and Physical Papers of G. G. Stokes*, Vol. 3, pp. 1–38. Johnson Reprint Corp., New York (1966).
21. S. TOMOTIKA, Laminar boundary layer on the surface of a sphere in a uniform stream, Br. Aero. Res. Comm., R and M, 1678 (1935).
22. D. B. SPALDING and C. CHI, Mass transfer through laminar boundary layers—4. Class I methods for predicting mass transfer rates. *Int. J. Heat Transfer* **6**, 363–385 (1963).
23. M. J. KAWAGUTI, An approximate solution for the slow viscous flow around a sphere, *Phys. Soc., Japan* **13**, 209 (1958).
24. L. J. SNYDER, T. W. SPRIGGS and W. E. STEWART, Solution of the equations of change by Galerkin's method *A.I.Ch.E. Jl* **10**, 535–540 (1964).
25. T. YUGE, Theory of heat transfer to spheres in a uniform stream at low Reynolds' numbers, *Rep. Iast. High Speed Mech., Tohoku Univ.* **6**, 143 (1956).
26. S. K. FRIEDLANDER, Mass and heat transfer to single spheres and cylinders at low Reynolds' numbers, *A.I.Ch.E. Jl* **3**, 43–48 (1957).
27. L. L. ROSS, Evaporation of droplets in a high temperature environment, Ph.D. Thesis, Chem. Eng. Dept. McMaster University (1966).
28. L. FOX, *Numerical Solution of Ordinary and Partial Differential Equations*, Chapt. 2. Pergamon Press, Oxford (1962).
29. J. M. MCCORMICK and M. G. SALVADOR, *Numerical Methods in Fortran*, Sec. 4–3. Prentice-Hall, New York (1964).
30. A. E. HAMIELEC, S. H. STOREY and S. M. WHITEHEAD, Viscous flow around spheres at intermediate Reynolds' numbers, *Can. J. Chem. Engng* **41**, 246–251 (1963).
31. R. KRUNIG and J. BRUIJSTEN, On the theory of heat and mass transfer from a sphere in a flowing medium at low values of Reynolds number, *Appl. Sci. Res.* **A2**, 439–446 (1951).
32. L. BREIMAN, Theory of heat and mass transfer from a steady moving sphere to the surrounding medium, Norman Bridge Laboratory, California Institute of Technology, Rept. No. 2F–2 (1952).
33. A. ACRIVOS and T. C. TAYLOR, Heat and mass transfer from single spheres in Stokes flow, *Physics Fluids* **5**, 387–394 (1962).
34. M. SIBULKIN, Heat transfer near forward stagnation point of a body of revolution, *J. Aero. Sci.* **19**, 570–571 (1952).
35. G. A. AKSEL-RUD, Diffusion from the surface of a sphere, *Zh. Prikl. Khim. Leningr.* **27**, 1446–1464 (1953).
36. KATSNEL'SON as reported in S. S. KUTATELADZE, *Fundamentals of Heat Transfer*, p. 242. Edward Arnold, London (1963).
37. C. BOWMAN, D. WARD, A. I. JOHNSON and O. TRASS, Mass transfer from fluid and solid spheres at low Reynolds numbers, *Can. J. Chem. Engng* **39**, 9–13 (1961).

APPENDIX A

Derivation of Expression for Nusselt Number

The complete energy equation, given by equation (10) may be arranged as follows,

$$\frac{2}{Pe}\left(\frac{\partial T}{\partial r}\right)_{r=1}\sin\theta\,\mathrm{d}\theta = \mathrm{d}\left[\int_0^y TV_\theta r\sin\theta\,\mathrm{d}r - \frac{2}{Pe}\int_1^y \frac{\partial T}{\partial\theta}\sin\theta\,\mathrm{d}r - \phi_A\sin\theta\,\mathrm{d}\theta.\right] \quad (A.1)$$

Integration of the local heat-transfer rate over the surface of the sphere yields the following expression for the Nusselt number,

$$Nu = \frac{2hR}{k} = -\int_0^{\pi}\left(\frac{\partial T}{\partial r}\right)_{r=1}\sin\theta\,d\theta. \tag{A.2}$$

Integration of equation (A.1), and using equation (A.2) results in

$$Nu = \frac{Pe}{2}\left[\int_1^y TV_\theta r\sin\theta\,dr - \frac{2}{Pe}\int_1^y \frac{\partial T}{\partial\theta}\sin\theta\,dr + \phi_A\cos\theta\right]_0^{\pi}. \tag{A.3}$$

Now at $\theta = 0$ we have

$$\left.\begin{aligned} &\int_1^y TV_\theta r\sin\theta\,dr = 0 \\ \text{also}\quad &\frac{2}{Pe}\int_1^y \frac{\partial T}{\partial\theta}\sin\theta\,dr = 0 \\ \text{and}\quad &\phi_A\cos\theta = \phi_A. \end{aligned}\right\} \tag{A.4}$$

Therefore equation (A.3) may be simplified to

$$Nu = \frac{Pe}{2}\left[\int_1^y TV_\theta r\sin\theta\,dr - \frac{2}{Pe}\int_1^y \frac{\partial T}{\partial\theta}\sin\theta\,dr - \phi_A(1-\cos\theta)\right]_{\theta=\pi} \tag{A.5}$$

or in terms of the transformed co-ordinates we have,

$$Nu = \left[x(2-x)q_1\,[q_2 + (1-x)q_3] - \frac{2}{Pe}\left(q_4\frac{dy}{dx}\right)_p\right]_{x=2} - Pe\,\phi_A \tag{A.6}$$

where, as discussed previously, the p subscript is used to denote a function evaluated from a preceding iteration solution.

Equation (A.6) is indeterminate at $x = 2$ (i.e. $\theta = 180$) for the case on non-separated flows: that is, $y \to \infty$ as $(2 - x) \to 0$. However, the Nusselt number asymptotically approaches a finite limit as $x \to 2$: thus, it may be obtained by extrapolation of values calculated close to the point of indeterminacy.

APPENDIX B

Thin Boundary-Layer Solution

Make the substitution, $l = y - 1$, into equation (10). Assume that the thermal boundary layer is thin so that $l \ll 1$. Furthermore assume that the upper limit on the mass efflux is dictated by the condition, $Pe\phi_A \ll 1/l$. With these assumptions the following simplification results

$$\int_1^y TV_\theta r\sin\theta\,dr \approx \frac{l^2}{10}\sin^2\theta(k_1 - k_2\cos\theta) \tag{B.1}$$

$$\text{where}\quad \left.\begin{aligned} k_1 &= 3A_{11} + 8A_{21} + 15A_{31} + 24A_{41} \\ k_2 &= 3A_{12} + 8A_{22} + 15A_{32} + 24A_{42}. \end{aligned}\right\} \tag{B.2}$$

It should be noted that if $\phi_A = 0$, k_1 and k_2 may be simplified from recursion formulas to

$$k_1 = \frac{(195 + 24A_{11})}{29} \tag{B.3}$$

$$k_2 = \frac{24}{27}A_{12}.$$

Now

$$-\left(\frac{\partial T}{\partial r}\right)_{r=1} + \frac{Pe\,\phi_A}{2} \approx \frac{3}{2l}. \tag{B.4}$$

Substitution of equations (B.1) and (B.2) into equation (10), neglecting the angular conduction term, yields, after re-arrangement,

$$\int_0^{\theta} d\left(\frac{l^2}{10}k_3\sin^2\theta\right) = \frac{3}{Pe}\int_0^{\theta}\frac{\sin\theta}{l}d\theta \tag{B.5}$$

$$\text{where}\quad k_3 = k_1 - k_2\cos\theta. \tag{B.6}$$

Note that

$$Nu_\theta = \frac{3}{2}\int_0^{\theta}\frac{\sin\theta}{l}d\theta \tag{B.7}$$

where Nu_θ is the Nusselt number based on the overall transfer from the sphere from $\theta = 0$ up to $\theta = \theta$.

Multiplying both sides of equation (B.5) by $l\sin\theta\,k^3/10$ yields,

$$\int_0^{k4} k_4^{\frac{1}{2}}\,d\,k_4 = \frac{3}{Pe}\frac{K_3^{\frac{1}{2}}\sin^2\theta}{10}d\theta \tag{B.8}$$

$$\text{where}\quad k_4 = l\sin\sqrt{\frac{k_3}{10}}. \tag{B.9}$$

$$\text{Therefore,}\ (k_4)^{\frac{3}{2}} = 0{\cdot}45\sqrt{10}\int_0^{\theta} k_2^{\frac{1}{2}}\sin^2\theta d\theta \tag{B.10}$$

Combining equations (B.7), (B.9) and (B.10) results in

$$Nu_\theta = \left(\frac{81}{160}Pe\right)^{\frac{1}{2}}\left(\int_0^{\theta} k_3^{\frac{1}{2}}\sin^2\theta\,d\theta\right)^{\frac{2}{3}} \tag{B.11}$$

Now $k_3 = 0$ denotes the condition for flow separation, since the separation angle, θ_s, is given by the relationship, $\theta_s = \cos^{-1}k_1/k_2$. As k_3 is negative for $\theta > \theta_s$, the Nusselt

number given by equation (B.11) may be evaluated up to $\theta = \theta_s$. Assume that the contribution to the energy transfer process from the region of separated flow is negligible with respect to the transfer prior to the separation point. Thus the overall Nusselt number is given as $Nu = Nu_{\theta s}$.

Thick Boundary-Layer Solution

For the case of thick boundary layers (i.e. $y \gg 1$), only the highest order term in equation (10), neglecting the angular conduction term, is significant and the equation may be reduced to,

$$\frac{\mathrm{d}}{\mathrm{d}\theta}\left[\frac{1}{16y^3}(-6y^4)\sin^2\theta\right] = -\frac{2}{Pe}\sin\theta. \tag{B.12}$$

Here we are considering only the case of zero mass efflux, i.e. $\phi_A = 0$.

Integration of equation (B.12) yields

$$y^2\sin^2\theta = -\frac{16\cos\theta}{3\,Pe} + \text{constant}. \tag{B.13}$$

Evaluating the arbitrary constant by applying the boundary $y = 1$ at $\theta = 0$ allows the equation to be written as

$$y = \frac{16}{3\,Pe}\frac{1}{(1+\cos\theta)} \tag{B.14}$$

but

$$\left(\frac{\partial T}{\partial r}\right)_{r=1} = \frac{2y+1}{2(1-y)}. \tag{B.15}$$

Substitution of equation (B.14) into (B.15) yields

$$\left(\frac{\partial T}{\partial r}\right)_{r=1} = \frac{32 + 3\,Pe(1+\cos\theta)}{6\,Pe(1+\cos\theta) - 32}. \tag{B.16}$$

Employing equation (B.16) in (A.2) results in

$$Nu = -\int_0^{\pi}\frac{[32 + 3\,Pe(1+\cos\theta)]}{6\,Pe(1+\cos\theta) - 32}\sin\theta\,\mathrm{d}\theta. \tag{B.17}$$

Equation (B.17) may be integrated directly. After rearrangement we have,

$$Nu = -1 - \frac{8}{Pe}\ln(1 - \tfrac{3}{8}Pe) \tag{B.18}$$

$$= 2 + \tfrac{9}{16}Pe + \tfrac{9}{64}Pe^2 + \ldots \tag{B.19}$$

which is the analytic solution sought.

ETUDE THÉORIQUE DE L'EFFET DU TRANSFERT MASSIQUE SUR LE TRANSFERT THERMIQUE POUR UNE GOUTTE EN COURS D'ÉVAPORATION

Résumé—On mène une recherche théorique sur l'interaction de l'écoulement radial résultant du transfert massique et de l'écoulement à convection forcée autour d'une goutte soumise à l'évaporation de façon à élucider l'effet du transfert massique sur le transfert thermique.

Le modèle théorique est basé sur:

(i) un flux massique uniforme autour de la goutte

(ii) une solution de l'équation de quantité de mouvement donnée par la fonction d'erreur

(iii) une formulation intégrale de l'équation d'énergie relative à la couche limite.

Les solutions pour le cas d'un flux massique nul recoupent les résultats rapportés antérieurement pour $0 < Re < 1000$. On a trouvé un excellent accord entre le modèle et les résultats expérimentaux utilisables qui correspondent à des flux massiques relativement élevés.

THEORETISCHE UNTERSUCHUNG DER AUSWIRKUNG DES MASSENTRANSPORTS AUF DEN WÄRMETRANSPORT AN EINEM VERDAMPFENDEN TROPFEN

Zusammenfassung—Es wurde eine theoretische Untersuchung über die Wechselwirkung zwischen der radialen Strömung des Massentransportes und dem Strömungsfeld der Zwangskonvektion um den verdampfenden Tropfen durchgeführt, um den Einfluss des Massentransportes auf den Wärmeübergang zu klären.

Die Grundlagen des theoretischen Modells sind

(1) gleichförmiger Massenstrom von der Tropfenoberfläche

(2) Fehlerverteilungsfunktion als Ansatz der Impulsgleichung

(3) Grenzschichtgleichung in integraler Form für die Energiegleichung.

Die Lösungen für verschwindenden Massenstrom stehen in guter Übereinstimmung mit früher veröffentlichten Beziehungen für $0 < Re < 1000$.

Es wurde hervorragende Übereinstimmung zwischen Modelluntersuchungen und den verfügbaren experimentellen Daten, die relativ hohe Massentransportströme überdecken, festgestellt.

ТЕОРЕТИЧЕСКОЕ ИССЛЕДОВАНИЕ ВЛИЯНИЯ МАССООБМЕНА НА ПЕРЕНОС ТЕПЛА К ИСПАРЯЮЩЕЙСЯ КАПЕЛЬКЕ

Аннотация—Теоретически исследовалось взаимодействие радиального, возникающего в результате переноса массы, и свободно-конвективного течения вокруг испаряющейся капельки в целях определения эффекта массообмена на теплообмен.

Теоретическая модель основывалась на:

(1) однородном истечении массы вокруг капельки;
(2) решении уравнения количества движения по методу распределения ошибки;
(3) интегральной формулировке уравнения для пограничного слоя.

Решения для случая нулевого истечения массы дали хорошее согласие с ранее докладываемыми корреляциями для $0 < Re < 1000$. Отличное соответствие получено между моделью и имеющимися экспериментальными данными для относительно больших скоростей массообмена.